

Optimal Tap Setting of Voltage Regulation Transformers Using Batch Reinforcement Learning

Hanchen Xu, *Student Member, IEEE*, Alejandro D. Domínguez-García, *Member, IEEE* and Peter W. Sauer, *Life Fellow, IEEE*

Abstract—In this paper, we address the problem of setting the tap positions of voltage regulation transformers—also referred to as the load tap changers (LTCs)—in radial power distribution systems under uncertain load dynamics. The objective is to find a policy that can determine the optimal tap positions that minimize the voltage deviation across the system, based only on the voltage magnitude measurements and the topology information. To this end, we formulate this problem as a Markov decision process (MDP), and propose a batch reinforcement learning (RL) algorithm to solve it. By taking advantage of a linearized power flow model, we propose an effective algorithm to estimate the voltage magnitudes under different tap settings, which allows the RL algorithm to explore the state and action space freely offline without impacting the real power system. To circumvent the “curse of dimensionality” resulted from the large state and action space, we propose a least squares policy iteration based sequential learning algorithm to learn an action value function for each LTC, based on which the optimal tap positions can be directly determined. Numerical simulations on the IEEE 13-bus and 123-bus distribution test feeders validated the effectiveness of the proposed algorithm.

Index Terms—voltage regulation, load tap changer, data-driven, Markov decision process, reinforcement learning.

I. INTRODUCTION

VOLTAGE regulation transformers—also referred to as load tap changers (LTCs)—are widely utilized in power distribution systems to regulate the voltage along the feeder. Conventionally, the tap position of each LTC is controlled through an automatic voltage regulator (AVR) based on local voltage measurements [1]. This approach, albeit simple and effective, is not optimal in any sense. Particularly, the voltage deviation may not be minimized. In the context of transmission systems, the transformer tap positions are optimized jointly with active and reactive power generation by solving the optimal power flow (OPF) problem, which are typically cast as mixed-integer programming problems (see, e.g., [2]–[4] and references therein). Similar OPF-based approaches are also adopted in power distribution systems. For example, in [5], Robbins et al. cast the optimal tap setting problem as a rank-constrained semidefinite program, which avoids the non-convexity and integer variables, and can thus be solved efficiently. This approach has also been widely applied in voltage control using distributed energy resources [6]–[9].

While these OPF-based approaches are effective in regulating voltages, they require complete system knowledge,

including active and reactive power injections, transmission/distribution line parameters, etc. While it may be reasonable to assume such information in transmission systems, the situation in distribution systems is quite different. Accurate line parameters may not be known and power injections at each bus may not be available in real-time, which prevents the application of the OPF-based approaches [10]–[12]. In addition, the OPF-based approaches typically deal with one snapshot of system conditions and assume loads remain constant between two snapshots. Therefore, the optimal tap setting problem needs to be solved for each snapshot in real-time.

In this paper, we develop a tap setting algorithm that can find a policy which determines the optimal tap positions under uncertain load dynamics using only voltage magnitude measurements and the topology information, without any information on power injections nor line parameters. Specifically, the optimal tap setting problem is cast as a multi-stage decision making problem modeled by a Markov decision process (MDP). The MDP can be solved using reinforcement learning (RL) algorithms, yet, adequate state and action samples that potentially cover most part in the state and action space are needed. However, this is hard to achieve in real power systems due to both security and economic concerns. To this end, we take advantage of a linearized power flow model and develop an effective algorithm to estimate the voltage under different tap settings so that the state and action space can be explored freely offline without impacting the real system. The state and action space increases exponentially as the number of LTCs grows, which causes the issue known as the “curse of dimensionality” and makes the computation intractable. To circumvent the “curse of dimensionality”, we propose an efficient batch RL algorithm—the least squares policy iteration (LSPI) based sequential learning algorithm—to learn an action value function sequentially for each LTC, based on which the optimal tap position of each LTC can be determined. We emphasize that the optimal policy can be computed offline, where the major computation happens, and when executed online, the required computation to find the optimal tap positions is trivial. We validated the effectiveness of the proposed algorithm through numerical simulations on the IEEE 13-bus and 123-bus distribution test feeders.

The remainder of the paper is organized as follows. Section II introduces a linearized power flow model that takes into account the impacts from LTCs. Section III reviews the basic concepts in MDP and RL, and briefly introduces the batch RL algorithm. The formulation of the optimal tap setting problem as an MDP is presented in Section IV, and the algorithms to

The authors are with the Department of Electrical and Computer Engineering at the University of Illinois at Urbana-Champaign, Urbana, IL 61801, USA. Email: {hxcu45, aledan, psauer}@illinois.edu.

solve it is detailed in Section V. Numerical simulation results on two IEEE test feeders are presented in Section VI. Section VII concludes the paper.

II. POWER DISTRIBUTION SYSTEM MODEL

In this section, we review a linearized power flow model for the distribution system and modify it to reflect the impacts from the LTCs.

A. Power Flow Model

Consider a power distribution network that consists of a set of buses indexed by the elements in $\tilde{\mathcal{N}} = \{0, 1, \dots, N\}$, and a set of transmission lines indexed by the elements in $\mathcal{L} = \{\ell := (i, j) : i, j \in \tilde{\mathcal{N}}\}$. Assume $|\mathcal{L}| = L$, where $|\cdot|$ denotes the cardinality of a set. Assume bus 0 is an ideal voltage source that corresponds to a substation bus, which is the only connection of the distribution system to a bulk power grid. Define $\mathcal{N} := \tilde{\mathcal{N}} \setminus \{0\}$.

Let V_i denote the magnitude of the voltage at bus i , $i \in \tilde{\mathcal{N}}$; V_0 is a constant since bus 0 is assumed to be an ideal voltage source. Define the square voltage magnitude as $u_i = V_i^2$, $i \in \tilde{\mathcal{N}}$. Let p_i and q_i denote the active power injection and reactive power injection at bus i , $i \in \mathcal{N}$, respectively. For each line $\ell \in \mathcal{L}$ that is associated with (i, j) , denote by p_{ij} and q_{ij} the respective active and reactive power flows on line (i, j) . Let r_ℓ and x_ℓ denote the resistance and reactance of line ℓ , $\ell \in \mathcal{L}$. For the radial distribution system, the relation between voltage magnitudes, power injections, and line power flows, can be captured by the so-called LinDistFlow model [13] as follows:

$$p_{ij} = -p_j + \sum_{k:(j,k) \in \mathcal{L}} p_{jk}, \quad (1a)$$

$$q_{ij} = -q_j + \sum_{k:(j,k) \in \mathcal{L}} q_{jk}, \quad (1b)$$

$$u_i - u_j = 2(r_\ell p_{ij} + x_\ell q_{ij}), \quad (1c)$$

where $\ell = (i, j)$.

Define $\mathbf{r} = [r_\ell]^\top$ and $\mathbf{x} = [x_\ell]^\top$, $\ell \in \mathcal{L}$. Let $\tilde{\mathbf{M}} = [\tilde{M}_{i\ell}] \in^{(N+1) \times L}$ denote the node-to-edge incidence matrix, with $\tilde{M}_{i\ell} = 1$ and $\tilde{M}_{j\ell} = -1$ if line $\ell = (i, j) \in \mathcal{L}$, and all other entries equal to zero. Let \mathbf{m}^\top denote the first row and \mathbf{M} the remaining $(N \times L)$ -dimensional matrix in $\tilde{\mathbf{M}}$. For a radial distribution system, $L = N$, and \mathbf{M} is invertible. Define $\mathbf{V} = [V_i]^\top$, $\mathbf{u} = [u_i]^\top$, $\mathbf{p} = [p_i]^\top$, and $\mathbf{q} = [q_i]^\top$, $i \in \mathcal{N}$. Then, the LinDistFlow model can be written in the vector form as follows:

$$\mathbf{M}^\top \mathbf{u} + \mathbf{m} u_0 = 2(\text{diag}(\mathbf{r})\mathbf{M}^{-1}\mathbf{p} + \text{diag}(\mathbf{x})\mathbf{M}^{-1}\mathbf{q}), \quad (2)$$

where $\text{diag}(\cdot)$ returns a diagonal matrix with the entries of the argument on its diagonals.

B. Load Tap Changer Model

We now introduce the model for the LTCs [5]. The classical model for a LTC is shown in Fig. 1, where $i = \sqrt{-1}$, $\ell = (i, j)$, and t_ℓ is the tap ratio of the LTC on line ℓ . Typically, the tap ratio can possibly take on 33 discrete values ranging

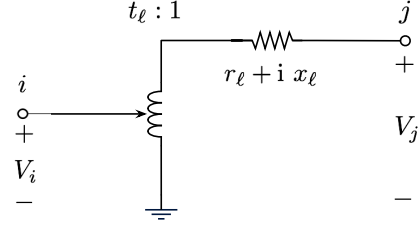


Fig. 1. Load tap changer model.

from 0.9 to 1.1, by an increment of 5/8% p.u. change, i.e., $t_\ell \in \mathcal{T} = \{0.9, 0.90625, \dots, 1.90375, 1.1\}$ [1]. We index the 33 tap positions by $-16, \dots, -1, 0, 1, \dots, 16$.

Let \mathcal{L}^t denote the set of lines with LTCs, and assume $|\mathcal{L}^t| = L^t$. Define $\mathbf{t} = [t_\ell]^\top$, $\ell \in \mathcal{L}^t$. In the case where line $\ell = (i, j) \in \mathcal{L}^t$, the voltage relation in LinDistFlow model, i.e. equation (1c), needs to be modified to the following:

$$\frac{1}{t_\ell^2} u_i - u_j = 2(r_\ell p_{ij} + x_\ell q_{ij}). \quad (3)$$

Let $\tilde{\mathbf{M}}^t = [\tilde{M}_{i\ell}^t] \in^{(N+1) \times L}$ denote the weighted node-to-edge incidence matrix, with $\tilde{M}_{i\ell}^t = 1$ and $\tilde{M}_{j\ell}^t = -1$ if line $\ell = (i, j) \in \mathcal{L} \setminus \mathcal{L}^t$, $\tilde{M}_{i\ell}^t = \frac{1}{t_\ell^2}$ and $\tilde{M}_{j\ell}^t = -1$ if line $\ell = (i, j) \in \mathcal{L}^t$, and all other entries equal to zero. Let $(\mathbf{m}^t)^\top$ denote the first row and \mathbf{M}^t the remaining $(N \times L)$ -dimensional matrix in $\tilde{\mathbf{M}}^t$. Then, the modified vector-form LinDistFlow model that takes into account the impacts from the LTCs is as follows:

$$(\mathbf{M}^t)^\top \mathbf{u} + \mathbf{m}^t u_0 = 2(\text{diag}(\mathbf{r})\mathbf{M}^{-1}\mathbf{p} + \text{diag}(\mathbf{x})\mathbf{M}^{-1}\mathbf{q}). \quad (4)$$

III. MARKOV DECISION PROCESS AND BATCH REINFORCEMENT LEARNING

In this section, we introduce the MDP, as well as the an data efficient and stable algorithm that solves the MDP problem, i.e., the batch RL algorithm. We use \mathbf{v}_k to denote the value of a vector \mathbf{v} at time step k and use $v_{i,k}$ to denote the value of the i^{th} entry of \mathbf{v} at time step k .

A. Markov Decision Process

A MDP consists of the following ingredients [14]: (i) a state space denoted by $\mathcal{S} = \{\mathbf{s}\}$, (ii) an action space denoted by $\mathcal{A} = \{\mathbf{a}\}$, (iii) a transition probability function $\pi(\mathbf{s}_{k+1}|\mathbf{s}_k, \mathbf{a}_k)$, (iv) a reward function $r : \mathcal{S} \times \mathcal{A} \mapsto \mathbb{R}$, and (v) a discount factor $\gamma \in [0, 1]$.¹ The transition probability function satisfies the Markov property, i.e.,

$$\pi(\mathbf{s}_{k+1}|\mathbf{s}_k, \mathbf{a}_k) = \pi(\mathbf{s}_{k+1}|\mathbf{s}_0, \mathbf{a}_0, \dots, \mathbf{s}_k, \mathbf{a}_k). \quad (5)$$

The total discounted reward from time instance k and onwards, denoted by R_k and referred to as the return, is

$$R_k = \sum_{k'=k}^{\infty} \gamma^{k'-k} r(\mathbf{s}_{k'}, \mathbf{a}_{k'}). \quad (6)$$

¹The discount factor γ can take the value of 1 only in episodic MDPs, i.e., MDPs that terminate within a finite number steps.

Under the Markov assumption, s_{k+1} is independent from $s_0, \mathbf{a}_0, \dots, s_{k-1}, \mathbf{a}_{k-1}$, conditioning on s_k and \mathbf{a}_k . Therefore, s_k contains all the necessary information to determine \mathbf{a}_k . Thus, the control policy μ can essentially be a mapping from s_k to \mathcal{A} . Specifically, a stochastic control policy is a mapping $\mu : \mathcal{S} \mapsto \mathcal{P}(\mathcal{A})$, where \mathcal{P} is some set of probability measure on \mathcal{A} ; a deterministic control policy is a mapping $\mu : \mathcal{S} \mapsto \mathcal{A}$.² The core problem of MDPs is the to find an optimal policy, denoted by μ^* , that maximizes the return R_k .

B. Action Value Function

MDPs can be solved by dynamic programming when the model is known and by RL algorithms when the model is unknown. The latter often relies on the action value function, which is also referred to as the Q-function. Intuitively, the Q-function quantifies how “good” the current state and action pair is in the long term. The Q-function under policy μ at action \mathbf{a} and state s , denoted by $Q^\mu(s, \mathbf{a})$, is defined to be the expected return as follows:

$$Q^\mu(s_k, \mathbf{a}_k) = \mathbb{E} [R_k | s_k, \mathbf{a}_k; \mu], \quad (7)$$

where $\mathbb{E}[\cdot]$ denotes the expectation. The action value function satisfies the following Bellman expectation equation:

$$Q^\mu(s, \mathbf{a}) = (B^\mu Q^\mu)(s, \mathbf{a}). \quad (8)$$

where B^μ is the Bellman operator:

$$(B^\mu Q^\mu)(s, \mathbf{a}) = \mathbb{E} [r(s, \mathbf{a})] \quad (9)$$

$$+ \gamma \sum_{s' \in \mathcal{S}} \pi(s' | s, \mathbf{a}) \sum_{\mathbf{a}' \in \mathcal{A}} \mu(\mathbf{a}' | s') Q^\mu(s', \mathbf{a}') \quad (10)$$

The Q-function under the optimal policy μ^* , denoted by $Q^*(\cdot, \cdot)$, satisfies the following Bellman optimality equation:

$$Q^*(s, \mathbf{a}) = \mathbb{E} [r(s, \mathbf{a})] + \gamma \sum_{s' \in \mathcal{S}} \pi(s' | s, \mathbf{a}) \max_{\mathbf{a}' \in \mathcal{A}} Q^*(s', \mathbf{a}'). \quad (11)$$

Given $Q^*(s, \mathbf{a})$, the greedy policy $\mu(s) = \arg \max_{\mathbf{a}} Q^*(s, \mathbf{a})$ is indeed an optimal policy.

When the state space and the action space are both discrete with small dimensions, the Q-function can be exactly represented using a table that covers the entire state and action space $\mathcal{S} \times \mathcal{A}$. In addition, the value of the Q-function can be computed using the Q-learning algorithm [15]. However, this approach cannot work when the state space or the action space has a high dimension or is continuous. In such situations, the Q-function is usually approximated by some parametric functions such as linear functions [16] and neural networks [17], or non-parametric functions such as decision trees or other kernel functions [18]. Yet, the Q-learning algorithm may diverge when function approximation is used.

²A deterministic control policy can be viewed as the limiting case of a stochastic policy.

C. Batch Reinforcement Learning

A type of data-efficient and stable algorithm that can address the aforementioned issue is the batch RL algorithms such as the LSPI algorithm [16]. Define the four-tuple $(s, \mathbf{a}, r(s, \mathbf{a}), s')$ as an experience and define a set of experience samples $\mathcal{D} = \{(s, \mathbf{a}, r(s, \mathbf{a}), s') : s, s' \in \mathcal{S}, \mathbf{a} \in \mathcal{A}\}$, where s' is the state following s after taking action \mathbf{a} . In batch RL algorithms, an approximate Q-function, denoted by $\hat{Q}(s, \mathbf{a})$, is fitted using experiences from \mathcal{D} via some regression algorithm.

Specifically, in the LSPI algorithm, $\hat{Q}(s, \mathbf{a})$ is assumed to be a function that is linear with respect to the parameters as follows:

$$\hat{Q}(s, \mathbf{a}) = \mathbf{w}^\top \phi(s, \mathbf{a}), \quad (12)$$

where $\phi(\cdot, \cdot) : \mathcal{S} \times \mathcal{A} \mapsto \mathbb{R}^f$ is a feature mapping for (s, \mathbf{a}) , which is also referred to as the basis function, $\mathbf{w} \in \mathbb{R}^f$ is the parameter vector. To emphasize the fact the $\hat{Q}(\cdot, \cdot)$ is parameterized by \mathbf{w} , we write $\hat{Q}(\cdot, \cdot)$ as $\hat{Q}^{\mathbf{w}}(\cdot, \cdot)$. At each iteration, the LSPI algorithm solves for a \mathbf{w} that minimizes the mean squared error between $\hat{Q}^{\mathbf{w}}(s, \mathbf{a})$ and projected $(B^{\mathbf{w}} \hat{Q}^{\mathbf{w}})(s, \mathbf{a})$ over \mathcal{D} .³ The algorithm iteratively improves the approximate Q-function by solving directly or recursively a least-squares regression problem, which has a closed-form solution. The convergence and performance guarantee of the LSPI algorithm is proved in [16].

IV. OPTIMAL TAP SETTING PROBLEM AS MDP

To effectively regulate the voltages in the power distribution system, the tap positions of LTCs need to be set appropriately. The objective of the optimal tap setting problem is to find a policy μ that determines from the voltage magnitudes the LTC tap ratios that minimize the voltage deviation from the reference value denoted by \mathbf{u}^* . Typically, $\mathbf{u}^* = \mathbf{1}_N$, where $\mathbf{1}_N$ is an all-ones vector in \mathbb{R}^N . We next formulate the optimal tap setting problem as an MDP.

1) *State Space*: Define the tap ratios and the squared voltage magnitudes at all buses but bus 0 as the state, i.e., $s = [\mathbf{t}^\top, \mathbf{u}^\top]^\top$, which has both continuous and discrete variables. Specifically, at time step k , the state is $s_k = [\mathbf{t}_{k-1}^\top, \mathbf{u}_k^\top]^\top$. The state space is $\mathcal{S} \subseteq \mathbb{R}^N \times \mathcal{T}^{L^t}$. Conventional Q-learning based approaches such as the ones in [19] and [20] only allow discrete values for the states, which necessitates discretization of the state space \mathcal{S} —the so-called state aggregation. In those approaches, the step size of the discretization is crucial. The discretized state space will better approximate the original state space if a small step size is used, yet the resulting MDP will face the “curse of dimensionality”. A large step size can alleviate the computational burden caused by the high dimension in the state space, but at the cost of potentially significant performance degradation. Applying function approximation allows us to handle any type of state variables.

³Note that the underlying policy, i.e., the greedy policy, is implicitly defined by \mathbf{w} ; therefore, we use the superscript \mathbf{w} in the Bellman operator.

2) *Action Space*: The action is the LTC tap ratios, i.e., $\mathbf{a} = \mathbf{t}$, and the action space is the set of all feasible values of LTC tap ratios, i.e., $\mathcal{A} = \mathcal{T}^{L_t}$. At time step k , the action is $\mathbf{a}_k = \mathbf{t}_k$. In the optimal tap setting problem, the action is discrete. The size of the action space increases exponentially with the number of LTCs. There is one LTC in the IEEE 13-bus distribution test feeder and four in the 123-bus distribution test feeder [21]. Since each LTC has 33 different tap ratios, the sizes of the action state for the IEEE 13-bus and 123-bus distribution test feeders are 33 and $33^4 = 1,185,921$.

3) *Reward Function*: The objective of voltage regulation is to minimize the voltage deviation. As such, we choose the reward function as

$$r(\mathbf{s}_k, \mathbf{a}_k) := -\frac{1}{N} \|\mathbf{u}_{k+1} - \mathbf{u}^*\|, \quad (13)$$

i.e., the immediate reward following action \mathbf{a}_k in state \mathbf{s}_k is the voltage deviation at time step $k+1$ after action \mathbf{a}_k is taken.

4) *Transition Probability Function and Discount Factor*: The remaining ingredients of the MDP are the transition probability function $\pi(\mathbf{s}_{k+1} | \mathbf{s}_k, \mathbf{a}_k)$ and the discount factor γ . The transition probability function are not known a priori, and in fact, is not necessary to know since the RL algorithm can learn from the experience samples. The discount factor is a parameter that can be chosen freely in $[0, 1]$. The larger γ is, the more future rewards are valued.

V. OPTIMAL TAP SETTING ALGORITHM

In this section, we propose a batch RL algorithm to solve the optimal tap setting problem. The proposed algorithm consists of an experience generating algorithm that can generate virtual experiences using existing historical data, and a LSPI-based sequential algorithm to solve the MDP. Some implementation details such as the feature selection are also discussed.

A. Overview

The overall structure of the optimal tap setting framework is illustrated in Fig. 2. The framework consists of an environment that is the power distribution system, a learning agent that learns the Q-function from a set of experience samples, and an acting agent that determines the optimal action from the Q-function. Specifically, the learning agent stores all the experience history in the set \mathcal{H} , and when needed, it will use a virtual experience generator to generate a set of experience samples denoted by \mathcal{D} based on the exploratory behavior defined in the exploratory actor. The set of experience samples is then used by a Q-function estimator, which is also referred to as the critic, to fit an approximate Q-function. The learning agent, which has a copy of the update-to-date approximate Q-function from the learning agent, finds a greedy action for the current state and instructs it to the LTCs.

Note that the learning of the Q-function can be done offline in the learning agent, which is capable to explore various system conditions through the virtual experience generator based on existing experience samples in \mathcal{H} , yet without directly interacting with the power distribution system. This avoids risking system security, which is a major concern of applying RL algorithms in power systems [22]. We will elaborate the details of the virtual experience generator in the next section.

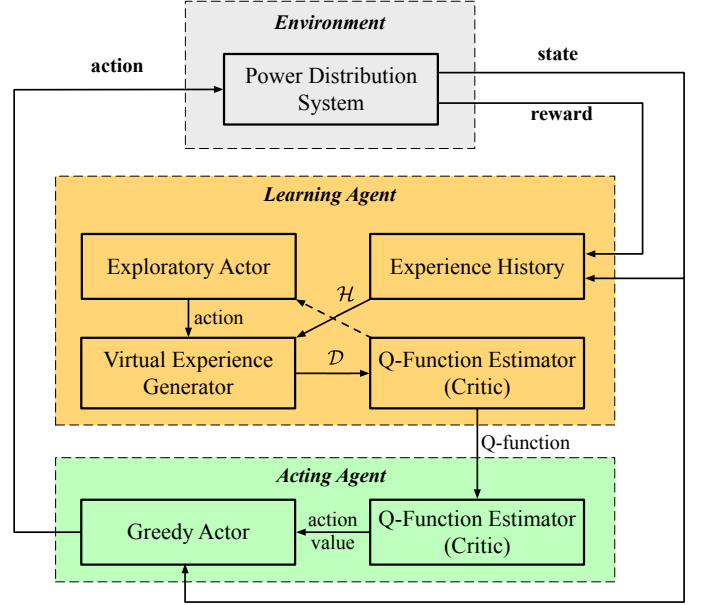


Fig. 2. The batch RL based framework for optimal tap setting.

B. Virtual Experience Generating

The RL algorithms are well-known to be demanding on data to achieve a good performance. The batch RL algorithms require adequate experience samples that spread over the state-action space $\mathcal{S} \times \mathcal{A}$. However, this is challenging in power systems since the system security may be at risk when exploring randomly. One way to work around with this issue is to use simulation models, rather than the physical system, to generate virtual experiences. To this end, we develop a data-driven virtual experience generator that simulate experiences without knowing the values of active and reactive power injections nor line parameters.

The fundamental idea is the following. When the tap ratios change while active and reactive power injections remain constant, the voltage magnitudes will change accordingly. Note that since the active and reactive power injections remain constant, then the right-hand-side in (4) does not change. Let the superscripts \dagger and \ddagger denote the prior- and post-tap-change value of a variable, respectively. Then, \mathbf{u}^\ddagger can be readily computed from \mathbf{u}^\dagger by solving the following linear equations:

$$(\mathbf{M}^{\mathbf{t}^\ddagger})^\top \mathbf{u}^\ddagger + \mathbf{m}^{\mathbf{t}^\ddagger} u_0 = (\mathbf{M}^{\mathbf{t}^\dagger})^\top \mathbf{u}^\dagger + \mathbf{m}^{\mathbf{t}^\dagger} u_0. \quad (14)$$

There are L equations and N variables in (14); therefore, it can be solved since $L = N$. The solution to (14) is the following:

$$\mathbf{u}^\ddagger = (\mathbf{M}^{\mathbf{t}^\dagger} (\mathbf{M}^{\mathbf{t}^\ddagger})^{-1})^\top \mathbf{u}^\dagger + ((\mathbf{M}^{\mathbf{t}^\ddagger})^\top)^{-1} (\mathbf{m}^{\mathbf{t}^\dagger} - \mathbf{m}^{\mathbf{t}^\ddagger}) u_0. \quad (15)$$

For ease of notation, we simply write (15) as

$$\mathbf{u}^\ddagger = \varphi(\mathbf{u}^\dagger, \mathbf{t}^\dagger, \mathbf{t}^\ddagger). \quad (16)$$

This nice property allows us to estimate the new values of voltage magnitudes when the tap positions change without knowing the exact values of active and reactive power injections and line parameters. The details of the virtual experience generating algorithm is presented in Algorithm 1.

Algorithm 1: Virtual Experience Generating**Input:**

\mathcal{H} : experience history set
 D : number of experience samples
 \mathbf{u}^* : reference value of squared voltage magnitudes
exploration policy

Output:

\mathcal{D} : experience sample set

Initialize experience sample set $\mathcal{D} \leftarrow \emptyset$

for $d = 1, \dots, D$ **do**

Choose from \mathcal{H} an experience sample ($\mathbf{s} = [\mathbf{t}^\top, \mathbf{u}^\top]^\top$, $\mathbf{a}^\dagger = \mathbf{t}^\dagger$, $r(\mathbf{s}, \mathbf{a}^\dagger)$, $\mathbf{s}^\dagger = [(\mathbf{t}^\dagger)^\top, (\mathbf{u}^\dagger)^\top]^\top$)
Select $\mathbf{a}^\ddagger = \mathbf{t}^\ddagger$ according to the exploration policy
Estimate \mathbf{u}^\ddagger following \mathbf{a}^\ddagger by $\mathbf{u}^\ddagger = \varphi(\mathbf{u}^\dagger, \mathbf{t}^\ddagger, \mathbf{t}^\ddagger)$
Estimate the reward as $r(\mathbf{s}, \mathbf{a}^\ddagger) = -\frac{1}{N} \|\mathbf{u}^\ddagger - \mathbf{u}^*\|$
Add $(\mathbf{s}, \mathbf{a}^\ddagger, r(\mathbf{s}, \mathbf{a}^\ddagger), (\mathbf{s}^\ddagger)^\dagger = [(\mathbf{t}^\ddagger)^\top, (\mathbf{u}^\ddagger)^\top]^\top)$ to \mathcal{D}

end

Algorithm 2: LSPI for Single LTC**Input:**

l : index of LTC
 D : experience sample set
 $\phi(\cdot, \cdot)$: basis function
 γ : discount factor
 ε : convergence threshold
 δ : pre-condition number

Output:

$\hat{Q}^{w^{(l)}}(\mathbf{s}, a_l)$: approximate Q-function for LTC l

Initialize $\mathbf{w}_1^{(l)} = \mathbf{w}_0^{(l)} = \mathbf{0}_f$ and $i = 1$

while $\|\mathbf{w}_i^{(l)} - \mathbf{w}_{i-1}^{(l)}\| > \varepsilon$ **do**

Initialize $\mathbf{A} = \delta \mathbf{I}_{f \times f}$ and $\mathbf{b} = \mathbf{0}_f$

for $(\mathbf{s}, \mathbf{a}, r(\mathbf{s}, \mathbf{a}), \mathbf{s}') \in \mathcal{D}$ **do**

Find the greedy action of LTC l for state \mathbf{s}' :

$$a'_l = \arg \max_a \hat{Q}^{w_k^{(l)}}(\mathbf{s}', a)$$

Update \mathbf{A} and \mathbf{b} by

$$\mathbf{A} \leftarrow \mathbf{A} + \phi(\mathbf{s}, a_l)(\phi(\mathbf{s}, a_l) - \gamma \phi(\mathbf{s}', a'_l))^\top$$

$$\mathbf{b} \leftarrow \mathbf{b} + r(\mathbf{s}, a_l) \phi(\mathbf{s}, a_l)$$

end

$$\mathbf{w}_{i+1}^{(l)} = \mathbf{A}^{-1} \mathbf{b}, i \leftarrow i + 1$$

end

C. LSPI based Sequential Q-function Learning

Given the experience sample set \mathcal{D} , we can now develop a learning algorithm for $\hat{Q}^w(\mathbf{s}, \mathbf{a})$ based on the LSPI algorithm (see [16]). While the LSPI is very efficient when the action space is relatively small, it becomes computationally intractable for large action space, since the number of unknown parameters in the approximate Q-function is typically proportional to $|\mathcal{T}^{L^t}|$, which increases exponentially with the number of LTCs. To overcome the ‘‘curse of dimensionality’’ that results from the action, we propose an LSPI based sequential learning algorithm to learn the Q-function.

The key idea is the following. Instead of learning an approx-

imate Q-function for the action vector \mathbf{a} , we learn a separate approximate Q-function for each component of \mathbf{a} , i.e., for each LTC $l = 1, \dots, L^t$, we learn an approximate Q-function $\hat{Q}^{w^{(l)}}(\mathbf{s}, a_l)$ that gives the value of the action component a_l in state \mathbf{s} . During the learning process of $\hat{Q}^{w^{(l)}}(\mathbf{s}, a_l)$, the rest of the LTCs are assumed to behave greedily according to their own approximate Q-function. To achieve this, we design the following exploration policy to generate the virtual experiences used when learning $\hat{Q}^{w^{(l)}}(\mathbf{s}, a_l)$ for LTC l . In the exploration step in Algorithm 1, the tap ratio of LTC l is selected uniformly in \mathcal{T} (uniform exploration), while those of others are selected greedily according to their up-to-date approximate Q-function (greedy exploration). Then, the LSPI algorithm that is detailed in Algorithm 2 is applied to learn $\hat{Q}^{w^{(l)}}(\mathbf{s}, a_l)$. These procedures are repeated for each LTC for J iterations. Using this LSPI based sequential learning algorithm, the total number of unknowns is then proportional to $L^t |\mathcal{T}|$, which is far fewer compared to $|\mathcal{T}^{L^t}|$ in the case where the approximate Q-function for the entire action vector \mathbf{a} is learned.

The tap setting algorithm works as follows. At time step k , a new state \mathbf{s}_k as well as the immediate reward following the action \mathbf{a}_{k-1} , $r(\mathbf{s}_{k-1}, \mathbf{a}_{k-1})$, is observed. The new experience $(\mathbf{s}_{k-1}, \mathbf{a}_{k-1}, r(\mathbf{s}_{k-1}, \mathbf{a}_{k-1}), \mathbf{s}_k)$ is added to \mathcal{H} . Every K time-steps, $\hat{Q}^{w^{(l)}}(\mathbf{s}, a_l)$, essentially $w^{(l)}$, for all $l = 1, \dots, L^t$, is updated by the learning agent by executing the LSPI based sequential learning algorithm, and the approximate Q-function in the acting agent is then synchronized. The acting agent then finds a greedy action for the current state \mathbf{s}_k and sends it to the LTCs. In order to reduce the wear and tear on the LTCs, the greedy action for the current state \mathbf{s}_k is not chosen if the difference between the action value resulting from the greedy action and that resulting from the current action is smaller than a threshold ϵ , i.e., the tap positions do not change in this case. The details of the optimal tap setting algorithm is given in Algorithm 3.

D. Implementation Details

A critical step in implementing the LSPI is constructing features from the state-action pair (\mathbf{s}, a_l) for LTC l . We use the radial basis functions (RBFs) as the basis function. The feature vector for a state-action pair (\mathbf{s}, a_l) , i.e., $\phi(\mathbf{s}, a_l)$, is a vector in \mathbb{R}^f , where $f = (\kappa + 1) \times |\mathcal{T}|$. $\phi(\mathbf{s}, a_l)$ has $|\mathcal{T}|$ segments, each with $\kappa + 1$ elements and corresponding a tap ratio in \mathcal{T} . Specifically, for $\mathbf{s} = [\mathbf{t}^\top, \mathbf{u}^\top]^\top$ and a_l that is the i^{th} tap ratio in \mathcal{T} , $\phi(\mathbf{s}, a_l)$ is computed as follows:

$$\phi(\mathbf{s}, a_l) = [0, \dots, 0, \underbrace{1, e^{-\frac{\|\mathbf{u}' - \bar{\mathbf{u}}_1\|}{\sigma^2}}, \dots, e^{-\frac{\|\mathbf{u}' - \bar{\mathbf{u}}_\kappa\|}{\sigma^2}}}_{i^{\text{th}} \text{ segment}}, 0, \dots, 0]^\top, \quad (17)$$

where $\sigma > 0$, $\mathbf{u}' = \varphi(\mathbf{u}, \mathbf{t}, \mathbf{t}')$, and $\bar{\mathbf{u}}_i$, $i = 1, \dots, \kappa$ are κ pre-specified constant vector in \mathbb{R}^N , referred to as the RBF centers.

The action a_l only determines which segment will be non-zero. \mathbf{t}' is obtained by replacing the l^{th} entry in \mathbf{t} with 1. Note that \mathbf{u}' is indeed the squared voltage magnitudes if the tap ratio

Algorithm 3: Optimal Tap Setting

Input:

K : approximate Q-function update period
 J : number of learning iterations
 ϵ : minimum action value change

for $k = 1, 2, \dots$ **do**

Observe the reward $r(\mathbf{s}_{k-1}, \mathbf{a}_{k-1})$ and the current state \mathbf{s}_k

Add $(\mathbf{s}_{k-1}, \mathbf{a}_{k-1}, r(\mathbf{s}_{k-1}, \mathbf{a}_{k-1}), \mathbf{s}_k)$ to \mathcal{H}

if $k \bmod K = 0$ **then** **for** $j = 1, \dots, J$ **do** **for** $l = 1, \dots, L^t$ **do**

 Run Algo. 1 to generate experience sample set \mathcal{D} using uniform exploration for LTC l and greedy exploration for other LTCs

 Run Algo. 2 to learn $\hat{Q}^{w^{(l)}}(s, a_l)$

end **end****end****for** $l = 1, \dots, L^t$ **do**

 Find the greedy action for LTC l :

if $\max_a \hat{Q}^{w^{(l)}}(s_k, a) - \hat{Q}^{w^{(l)}}(s_k, a_{l,k-1}) > \epsilon$ **then**

$a_{l,k} = \arg \max_a \hat{Q}^{w^{(l)}}(s_k, a)$

else

$a_{l,k} = a_{l,k-1}$

end**end**

 Adjust the LTC tap ratios to \mathbf{a}_k

end

of LTC l is at the nominal value 1.0. Each RBF computes the distance between \mathbf{u}' and some pre-specified squared voltage magnitudes.

VI. NUMERICAL SIMULATION

In this section, we apply the proposed algorithm to the IEEE 13-bus and 123-bus test feeders.

A. Simulation Setup

The loads for both these two test feeders are simulated based on historical hourly load data from a residential building in San Diego [23]. Specifically, the historical active power load data are scaled to match the active power load level in the particular distribution test feeder and interpolated to increase the time granularity to 5 minutes. The total active power load is then proportionally redistributed to each load bus, with some added noise. Each load bus is assumed to have a constant power factor of 0.95.

We first verify the accuracy of the virtual experience generating algorithm. Specifically, assume the voltage magnitudes are known for some unknown loads under a known tap ratio of 1. We define the voltage approximation error for a certain tap position to be the absolute difference between the true and the estimated voltage magnitude. The voltage approximation

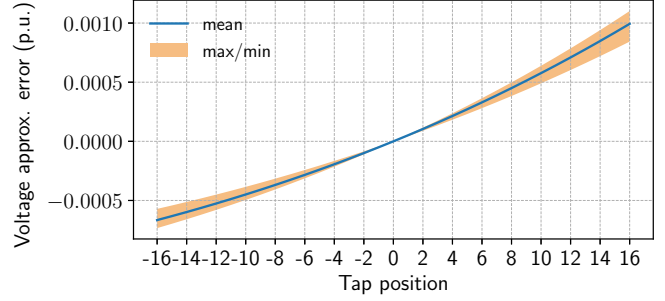


Fig. 3. Voltage approximation error. (Position 0 corresponds to tap ratio 1.)

error for the IEEE 13-bus test feeder is presented in Fig. 3. As shown in Fig. 3, the maximum approximation error is smaller than 0.001 p.u., which is accurate enough. The result for the IEEE 123-bus test feeder is similar.

B. Case Study on IEEE 13-bus Test Feeder

We first illustrate the proposed algorithm in the IEEE 13-bus test feeder to get some insights into this algorithm. In the simulation, 21 RBF centers are used, i.e., $\kappa = 21$. Specifically, $\bar{\mathbf{u}}_i = (0.895 + 0.005i)^2 \times \mathbf{1}_N$. The policy is updated every 2 hours, i.e., $K = 24$, which corresponds to two hours. The 120 actual experiences over the same time interval in the previous 5 days, where the LTC tap ratio is 1, are used to generate $D = 6000$ virtual experiences. Since this test feeder only has one LTC, there is no need to sequentially update the approximate Q-function, so we set $J = 1$. Other parameters are chosen as follows: $\mathbf{u}^* = \mathbf{1}_N$, $\gamma = 0.9$, $\varepsilon = 1 \times 10^{-5}$, $\epsilon = 1 \times 10^{-4}$, $\delta = 0.1$, and $\sigma = 1$.

Assuming complete and perfect knowledge on the system parameters as well as active and reactive power injections for all time steps, we can find the optimal tap position that results in the highest immediate reward by exhaustively searching the action space, i.e., all feasible tap ratios, at each time step. It is important to point out that, in practice, the exhaustive search approach is infeasible since we do not have the necessary information, and not practical due to the high computation burden. Results obtained by the exhaustive search approach, and results obtained under nominal tap ratio, are used to benchmark the proposed algorithm.

Figure 4 shows the voltage magnitude profiles under the optimal tap setting algorithm. The voltage magnitude profiles under the proposed batch RL approach are quite similar to the those obtained via the exhaustive search approach, both shows significant improvement over those under the nominal tap ratio. Figure 5 shows the tap positions and the immediate rewards under different approaches. The tap positions under the batch RL approach and the exhaustive search approach are aligned during most of the time in the day. Note that while the LTC has 33 tap positions, only a small portion of them will be actually used. This motivates us to further reduce the action space by narrow the action space to a smaller range. The immediate rewards resulted from these two approaches are very close. The mean immediate rewards obtained by the

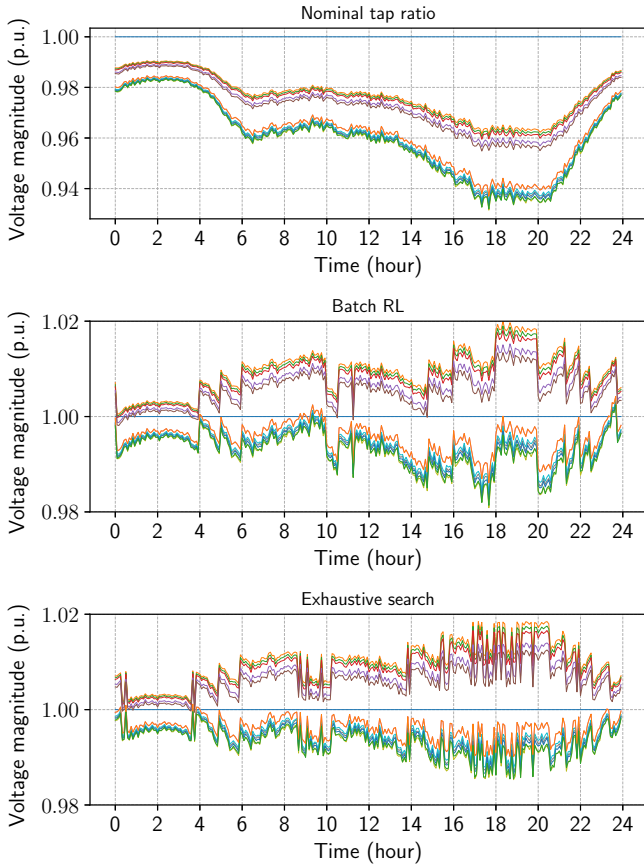


Fig. 4. Voltage magnitude profiles of IEEE 13-bus distribution test feeder.

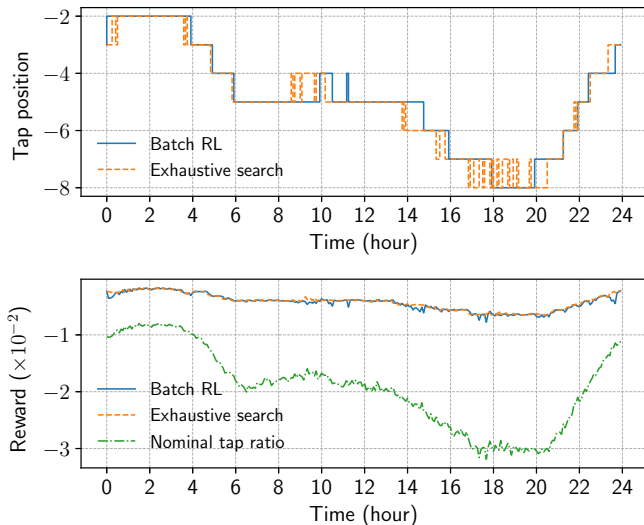


Fig. 5. Tap positions and immediate rewards for IEEE 13-bus test feeder.

batch RL approach and the exhaustive search approach are -4.279×10^{-3} and -4.156×10^{-3} , respectively, while that under the nominal tap ratio is -19.26×10^{-3} . We also would like to point out that Algorithm 2 typically converges within 5 iterations within 20 seconds, and the batch RL approach is faster than the exhaustive search approach by several orders

TABLE I
REWARDS UNDER VARIOUS POLICY UPDATE PERIODS.

update period (hour)	2	4	6	8	24
reward mean ($\times 10^{-3}$)	-4.279	-4.290	-4.390	-4.347	-4.501
reward std. ($\times 10^{-3}$)	1.436	1.423	1.480	1.529	1.601

of magnitude.

While the policy in the above simulation is learnt using data over 2 hours, it is also feasible to learn using data over a longer period. Table I shows the mean and standard deviation (std.) of the immediate reward over one day when the policy is learnt using data over different periods, when the actual experiences are enhanced by 50 times. As can be seen, the resulting rewards do not vary too much. Yet, learning a policy using data over a shorter period typically reduces the requirement amount of data, while achieving a equally good (or even better) result.

C. Case Study on IEEE 123-bus Test Feeder

We next test the proposed algorithm on the IEEE 123-bus test feeder. Motivated by the results in the smaller case, the action space of the LTCs in this case are narrowed to a smaller space. We allow 9 positions from -8 to 0 for two LTCs, and 5 positions from 0 to 5 for the other two LTCs. 11 RBF centers are used, i.e., $\kappa = 11$. Specifically, $\bar{\mathbf{u}}_i = (0.94 + 0.01i)^2 \times \mathbf{1}_N$ for all LTCs except for the one near the substation, for which $\bar{\mathbf{u}}_i = (0.89 + 0.01i)^2 \times \mathbf{1}_N$. The 120 actual experiences over the same time interval in the previous 5 days, where the LTC tap ratio is 1, are used to generate $D = 3600$ virtual experiences. The number of iterations in the LSPI based sequential learning algorithm is set to $J = 3$. Other parameters are the same as in the previous section.

Figure 6 shows the tap positions and immediate rewards under different approaches. The mean reward obtained by the batch RL approach and the exhaustive search approach are -1.646×10^{-3} and -1.402×10^{-3} , respectively, while that under the nominal tap ratio is -7.513×10^{-3} . While the tap positions differs, the immediate rewards resulted from these two approaches are very close. Note that the tap changes are smoother in the proposed approach since we have enforced a minimum Q-function change requirement to trigger a tap change action.

Figure 7 shows the immediate rewards over one week. As can be seen from Fig. 7, the voltage regulation performance achieved by the proposed algorithm is in general close to that achieved by the exhaustive search approach. Due to the space limitation, other simulation results such as voltage profiles are not presented here.

VII. CONCLUDING REMARKS

In this paper, we formulated the optimal tap setting problem of LTCs as an MDP and proposed a batch RL algorithm to solve it. To obtain adequate state action samples, we develop a virtual experience generating algorithm that estimates the voltage magnitudes under different tap settings. To circumvent

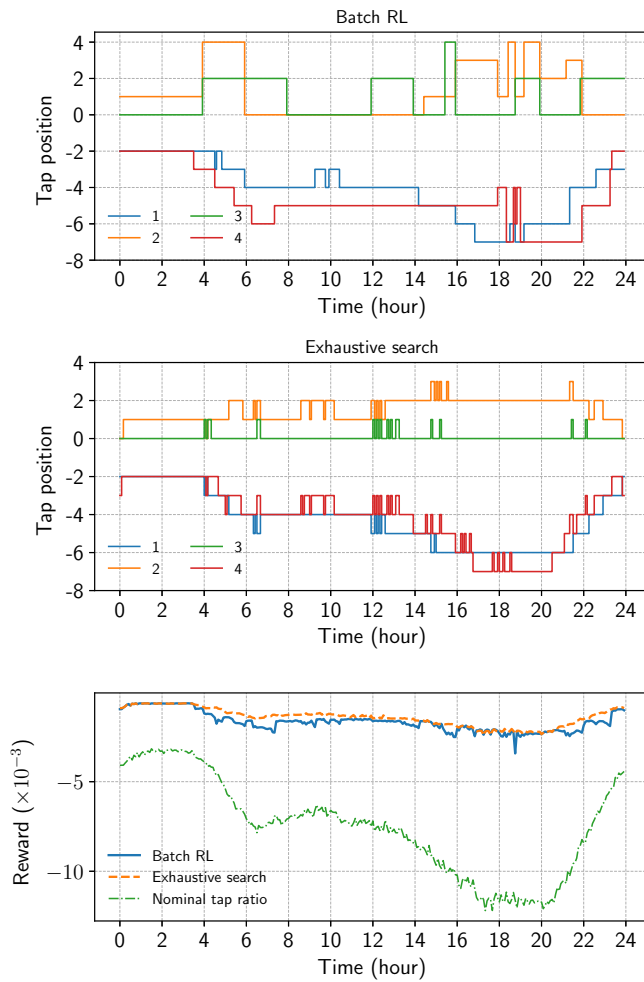


Fig. 6. Tap positions for IEEE 123-bus test feeder.

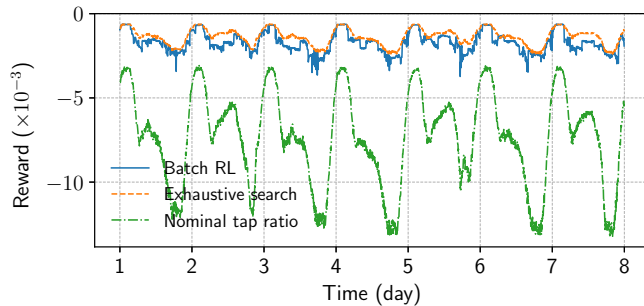


Fig. 7. Immediate rewards for IEEE 123-bus test feeder over 7 days.

the “curse of dimensionality”, we proposed an LSPI based sequential learning algorithm to learn an action value function for each LTC, based on which the optimal tap positions can be determined directly. The proposed algorithm can find the policy that determines the optimal tap positions that minimize the voltage deviation across the system, based only on the voltage magnitude measurements and the topology information, which makes it more desirable for implementation in practice. Numerical simulation on the IEEE 13-bus and 123-bus test

feeders validated the effectiveness of the proposed batch RL based algorithm.

REFERENCES

- [1] P. Kundur, N. J. Balu, and M. G. Lauby, *Power system stability and control*. McGraw-hill New York, 1994, vol. 7.
- [2] W. H. E. Liu, A. D. Papalexopoulos, and W. F. Tinney, “Discrete shunt controls in a newton optimal power flow,” *IEEE Trans. Power Syst.*, vol. 7, no. 4, pp. 1509–1518, Nov 1992.
- [3] M. R. Salem, L. A. Talat, and H. M. Soliman, “Voltage control by tap-changing transformers for a radial distribution network,” *IEE Proceedings - Generation, Transmission and Distribution*, vol. 144, no. 6, pp. 517–520, Nov 1997.
- [4] Z. Yang, A. Bose, H. Zhong, N. Zhang, Q. Xia, and C. Kang, “Optimal reactive power dispatch with accurately modeled discrete control devices: A successive linear approximation approach,” *IEEE Trans. Power Syst.*, vol. 32, no. 3, pp. 2435–2444, May 2017.
- [5] B. A. Robbins, H. Zhu, and A. D. Domínguez-García, “Optimal tap setting of voltage regulation transformers in unbalanced distribution systems,” *IEEE Trans. Power Syst.*, vol. 31, no. 1, pp. 256–267, Jan 2016.
- [6] H. Zhu and H. J. Liu, “Fast local voltage control under limited reactive power: Optimality and stability analysis,” *IEEE Trans. Power Syst.*, vol. 31, no. 5, pp. 3794–3803, Sept. 2016.
- [7] B. Zhang, A. Y. S. Lam, A. D. Domínguez-García, and D. Tse, “An optimal and distributed method for voltage regulation in power distribution systems,” *IEEE Trans. Power Syst.*, vol. 30, no. 4, pp. 1714–1726, July 2015.
- [8] B. A. Robbins and A. D. Domínguez-García, “Optimal reactive power dispatch for voltage regulation in unbalanced distribution systems,” *IEEE Trans. Power Syst.*, vol. 31, no. 4, pp. 2903–2913, July 2016.
- [9] V. Kekatos, G. Wang, A. J. Conejo, and G. B. Giannakis, “Stochastic reactive power management in microgrids with renewables,” *IEEE Trans. Power Syst.*, vol. 30, no. 6, pp. 3386–3395, Nov 2015.
- [10] H. Xu, A. D. Domínguez-García, and P. W. Sauer, “A data-driven voltage control framework for power distribution systems,” in *Proc. of IEEE PES General Meeting*, Portland, OR, Aug. 2018, pp. 1–5.
- [11] —, “Adaptive coordination of distributed energy resources in lossy power distribution systems,” in *Proc. of IEEE PES General Meeting*, Portland, OR, Aug. 2018, pp. 1–5.
- [12] —, “Data-driven coordination of distributed energy resources for active power provision,” *arXiv preprint arXiv:1804.00043*, 2018.
- [13] M. E. Baran and F. F. Wu, “Network reconfiguration in distribution systems for loss reduction and load balancing,” *IEEE Trans. Power Del.*, vol. 4, no. 2, pp. 1401–1407, Apr 1989.
- [14] R. S. Sutton and A. G. Barto, *Reinforcement learning: An introduction*. MIT press Cambridge, 1998, vol. 1, no. 1.
- [15] C. J. Watkins and P. Dayan, “Q-learning,” *Machine learning*, vol. 8, no. 3-4, pp. 279–292, 1992.
- [16] M. G. Lagoudakis and R. Parr, “Least-squares policy iteration,” *Journal of machine learning research*, vol. 4, no. Dec, pp. 1107–1149, 2003.
- [17] V. Mnih, K. Kavukcuoglu, D. Silver, A. A. Rusu, J. Veness, M. G. Bellemare, A. Graves, M. Riedmiller, A. K. Fidjeland, G. Ostrovski *et al.*, “Human-level control through deep reinforcement learning,” *Nature*, vol. 518, no. 7540, p. 529, 2015.
- [18] D. Ernst, P. Geurts, and L. Wehenkel, “Tree-based batch mode reinforcement learning,” *Journal of Machine Learning Research*, vol. 6, no. Apr, pp. 503–556, 2005.
- [19] J. G. Vlachogiannis and N. D. Hatziargyriou, “Reinforcement learning for reactive power control,” *IEEE Trans. Power Syst.*, vol. 19, no. 3, pp. 1317–1325, 2004.
- [20] Y. Xu, W. Zhang, W. Liu, and F. Ferrese, “Multiagent-based reinforcement learning for optimal reactive power dispatch,” *IEEE Trans. Syst., Man, Cybern., Syst., Part C (Applications and Reviews)*, vol. 42, no. 6, pp. 1742–1751, 2012.
- [21] IEEE distribution test feeders. [Online]. Available: <https://ewh.ieee.org/soc/pes/dsaom/testfeeders/>
- [22] M. Glavic, R. Fonteneau, and D. Ernst, “Reinforcement learning for electric power system decision and control: Past considerations and perspectives,” *IFAC-PapersOnLine*, vol. 50, no. 1, pp. 6918–6927, 2017.
- [23] Commercial and residential hourly load profiles for all TMY3 locations in the United States. [Online]. Available: <https://openepi.org/doe-opendata/dataset>